Metal/Fluorocarbon Pyrolants: VI. Combustion Behaviour and Radiation Properties of Magnesium/Poly(Carbon Monofluoride) Pyrolant

Ernst-Christian Koch*

Diehl BGT-Defence GmbH & Co. KG, Fischbachstrasse 16, D-90552 Röthenbach a. d. Pegnitz (Germany)

Dedicated to Dr. Bernard E. Douda on the occasion of his 75th birthday

Abstract

The performance of poly(carbon monofluoride) (PMF) (synonym: graphite fluoride) $(CF_x)_n$, (**1**) as oxidizer in a fuel rich Mg based pyrolant ($\xi(Mg) = 0.45$) is investigated. The radiance [W sr^{-1}] under both static and dynamic conditions, the spectral radiant exitance [W cm^{-2} μm^{-1}], the linear burn rate [mm s^{-1}] and the mass consumption rate [g s^{-1} cm^{-2}] have been determined. Calculations for enthalpy of anaerobic and aerobic combustion [kJ g^{-1}] and for the equilibrium composition of the combustion products as well as combustion temperature are given. A mechanism for the reaction is discussed. The combustion product from $Mg/(CF_x)_n$ surprisingly reveals the formation of single walled carbon nanotubes (SWCNT) and "carbon nano carpet rolls" (CNCR). For part V see Ref. [1].

Keywords: Graphite Fluoride, Infrared Radiance, Magnesium, Nanotubes, Poly(carbon monofluoride), Pyrolant

1 Introduction

Pyrolant systems based on magnesium/polytetrafluoroethylene (Teflon™)/hexafluoropropylene vinylidene fluoride copolymer (Viton™) (MTV) are the major payloads applied in aerial infrared decoy flares [2]. Aside from application in infrared decoy flares MTV finds also application in civilian and military devices such as airbag igniters and rocket motor igniters [3].

The radiative properties of MTV pyrolants have been investigated by numerous researchers under both static [4–6] and dynamic conditions [7], as well as in vacuum [8]. Alekeseev has recently modelled the spectral radiant exitance of MTV based on the radiation transfer equations and gas dynamic considerations [9]. In terms of specific intensity E_λ, [J g^{-1} sr^{-1}] MTV is superior to many other pyrolant systems applied so far. In 1999 the author found poly(carbon monofluoride) to act as a sole oxidizer superior to PTFE in metal based pyrolant systems [10].

* E-mail: ernst.christian.koch@diehl-bgt-defence.de

2 Poly(Carbon Monofluoride)

Poly(carbon monofluoride) (PMF) (synonym: graphite fluoride)(**1**), a crystalline solid layered fluorocarbon having the approximate formula (CF_x) with x = ranging from 0.08 to 1.17 was first applied as combustion modifier to boron based propellants by Liu and co-workers in 1993. Liu et al. recognized the mode of action of PMF in that it yields highly reactive fluorinated specie difluorocarbene ($:CF_2$) upon thermal decomposition. Difluorocarbene attacks the oxide coating of boron particles and accelerates the combustion by removing it according to Eq. (1) [11, 12].

$$B_2O_3 + 3 : CF_{2(g)} \xrightarrow{\Delta} 2\ BF_{3(g)} + 3\ CO_{(g)} + 1785\ kJ \qquad (1)$$

At the time of writing this paper an older US patent application from 1977 which had been kept secret has been released. It teaches the application of graphite fluoride as preferred oxidizer in air-augmented ramjet engines together with Al and Carboxy-Terminated-PolyButadiene (CTPB). Although the patent explicitly refers to compound (**1**) the advantageous thermochemical properties of graphite fluoride compared to poly(tetrafluoroethylene) have not been considered there [13]. Fig. 1 shows a typical TEM picture of PMF (**1**) particles.

Table 1 compares the thermochemical properties of poly(tetrafluoroethylene)(PTFE) (**2**), poly(carbon monofluoride) (PMF) (**1**) and common binder Viton™ (**3**) that is hexafluoropropylene vinylidene fluoride copolymer.

3 Thermochemical Properties of Poly(Carbon Monofluoride)

The enthalpy of formation of acyclic, saturated fluorocarbons, CF_x, can be approximated using the functional linear relationship given in Eq. (2) [14].

$$\Delta_f H^\circ(CF_x) = (-257.99 \cdot x + 93.30)\ kJ \cdot mol^{-1} \qquad (2)$$

 DOI: 10.1002/prep.200500007

Table 1. Properties of fluorocarbon polymers

Parameter	Unit	**2**	**1**	**3**
Name		Poly(tetrafluoroethylene)	Poly(carbon monofluoride)	Hexafluoropropylene vinylidene fluoride copolymer
CAS-Nr.		9002-84-0	11113-63-6	9011-17-0
Constitution		$(-C_2F_4-)_n$	$(CF_x)_n$	$(-CF(CF_3)CF_2-)_n(-CH_2CF_2-)_m$
m_r	g mol^{-1}	100.02	31.01 at x = 1	374.145
Aspect		off-white	off-white to brown depending on x	translucent
$\rho_{20\,^\circ C}$	g·cm^{-3}	2.31	2.65 at x = 1	1.85
T_{mp}	°C	324	480, decomp., at x = 1	decomp.
T_{bp}	°C	decomp.	n.a.	decomp.
$\Delta_f H^\circ$	kJ mol^{-1}	-809	−196 at x = 1	−2784
c_t	W m^{-1} K^{-1}	0.244	n.a.	0.13
C_{p298K}	J g^{-1} K^{-1}	1.02	0.89 at x = 1	1.3
$\Delta_m H^\circ$	kJ mol^{-1}	-3.6	n.a.	n.a.
$\Delta_d H^\circ$	kJ mol^{-1}	-172	n.a.	−128

m_r: molecular weight; $\rho_{20\,^\circ C}$: density at 20 °C; T_{mp}: melting point; T_{bp}: boiling point; $\Delta_f H$: enthalpy of formation; c_t: thermal conductivity; C_{p298K}: specific heat; $\Delta_m H$: enthalpy of fusion, $\Delta_d H$: enthalpy of decomposition

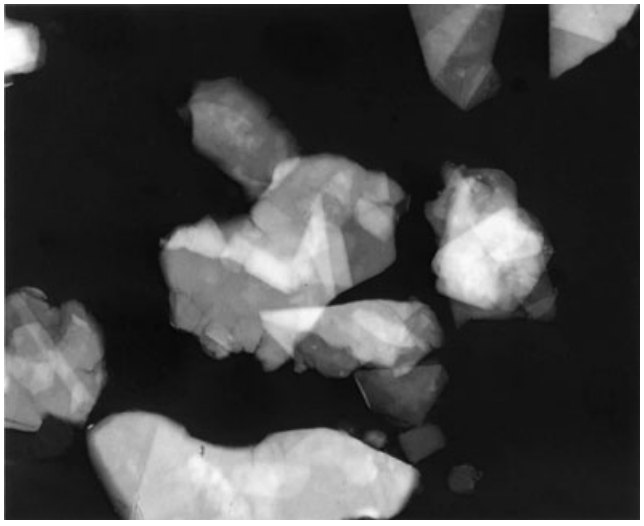

Figure 1. TEM picture of poly(carbon monofluoride) (**1**)

Eq. (2) describes that the enthalpy of formations of a fluorocarbon compound increases with increasing number of fluorine atoms attached to a single carbon atom.

Considering stoichiometric mixtures the following equations explain for the increased exothermicity of PMF based systems compared to those based on PTFE [15]:

$$\overbrace{2Mg}^{0} + \frac{4}{m}\overbrace{C_nF_m}^{\Delta_f H^\circ} \longrightarrow 2\overbrace{MgF_2}^{-1124} + \frac{4\cdot n}{m}\overbrace{C}^{0} \tag{3}$$

$$\begin{aligned} \Delta_f H^\circ(-C_2F_4-)_n &= -809\ \text{kJ}\cdot\text{mol}^{-1}, \\ \Delta_c H((-C_2F_4-)_n/Mg) &= -1438\ \text{kJ}\cdot\text{mol}^{-1} \end{aligned}$$

$$\begin{aligned} \Delta_f H^\circ(CF)_n &= -196\ \text{kJ}\cdot\text{mol}^{-1}, \\ \Delta_c H((CF)_n/Mg) &= -1468\ \text{kJ}\cdot\text{mol}^{-1} \end{aligned}$$

The thermal decomposition of poly(carbon monofluoride) has been investigated early by Watanabe [16]. Thus under nitrogen at $T = 600\,^\circ C$ the following mechanism is discussed, following a cubic law:

$$\left(\frac{2x+3y}{n}\right)(CF)_n \xrightarrow{\Delta} (x+2y)C + x:CF_2 + yC_2F_4 \tag{4}$$

Considering a reductive environment, that is the presence of an electron donor such as magnesium, the surface fluorine atoms can react with magnesium to give the reactive intermediate (**I**) given in Eq. (5) [1].

$$n\text{Mg} + (\text{CF})_n \xrightarrow{\Delta} \underset{(\mathbf{I})}{(\text{C}-\text{Mg}-\text{F})_n},\ \ \Delta H < 0 \tag{5}$$

Further heat accumulation and presence of available fluorine atoms trigger the exothermal elimination of MgF_2 according to:

$$(\text{CF})_n + \underset{(\mathbf{I})}{(\text{C}-\text{Mg}-\text{F})_n} \xrightarrow{\Delta} 2n\text{C} + \text{MgF}_2,\ \ \Delta H < 0 \tag{6}$$

The latter reaction provides the necessary heat to initiate the thermal decomposition of the graphite fluoride.

3.1 DSC Investigation of the Pyrolant

A pyrolant was made from 55 wt-% graphite fluoride, 40 wt-% magnesium and 5 wt-% Viton^{TM} by dissolving Viton (purchased as Fluorel FC-2175 from MACH I Inc. / King of Prussia, USA) in Acetone (purchased from MERCK, Darmstadt, Germany) and successive mixing with magnesium (purchased as LNR 61 grade from ECK-ART Metallwerke, St. Georgen, Austria; particle distribution: 11% >63 μm, 53% 63–40 μm, 36% <40 μm) and

finally poly(carbon monofluoride) (purchased as product no. 37,245-5 from Sigma-Aldrich, Taufkirchen, Germany; particle size: 400 mesh, F-content by weight >61%). The mixture was stirred in an air stream to allow for evaporation of acetone to yield a crumbling mass. This was passed through a 2.5 mm sieve and dried in a constant air-stream at 40 °C for 30 min. The dried granules were then pressed in a die providing 23 × 19 mm in square geometry giving a strand of a total of 95 g having a final density of 1.876 g cm^{-3} that is 88.5% of a theoretical maximum density (TMD) of 2.12 g cm^{-3}.

This pyrolant was cut into small pieces weighing between 4–6 mg. These pieces were investigated by means of DSC (Mettler Toledo, DSC 20, Argon (5.9) flow: 50 ml min^{-1}) The samples were placed in doubly perforated closed aluminium crucibles and measured at heating rates: 5, 10, 15, 20 and 50 K min^{-1}. Fig. 2 displays the experiments.

In Fig. 2 at 5 K min^{-1} an exothermal (T_{max} = 584 °C) with a distinct shoulder at 568 °C is seen. At 10 K min^{-1} heating rate, only a single slightly broadened exothermal is seen (T_{max} = 556 °C). Increasing the heating rate to 15 K min^{-1} reveals two exothermals giving a broad signal at 502 °C and another one at T > 600 °C. At a heating rate of 20 K min^{-1}, the lower temperature exothermal is resolved as a sharp signal with T_{max} = 521 °C. At even higher heating rates, the exothermal shifts to higher temperature (T_{max} = 549 °C).

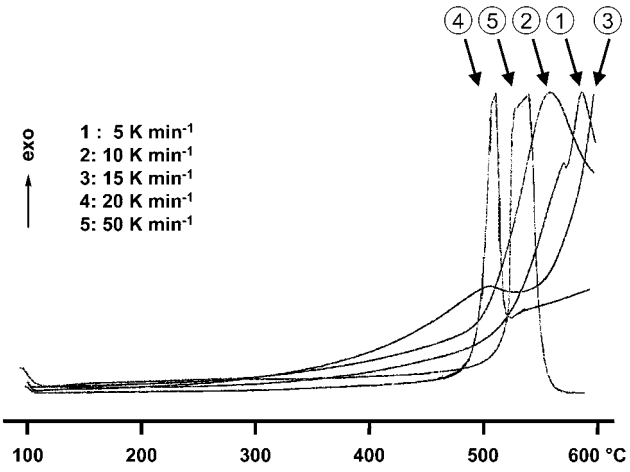

Figure 2. DSC plots of pyrolant at 5, 10, 15, 20 and 50 K min^{-1}.

The original pyrolant was investigated by means of FTIR-spectroscopy (Perkin Elmer 1630). Therefore the solid material was ground in a mortar and mixed with anhydrous potassium bromide. Fig. 3 displays IR spectra for pristine pyrolant and pyrolant after heating to 510 and 600 °C respectively.

The lowest trace shows only tertiary C-F vibration at a wave number of $\bar{\nu}$ =1150 cm^{-1}.

The second trace (510 °C) still shows tertiary C-F vibration but also low intense vibrations at both higher and lower wave numbers indicating the formation of new C-F species. The small signal at $\bar{\nu}$ =560 cm^{-1} is indicative of Mg-C bond

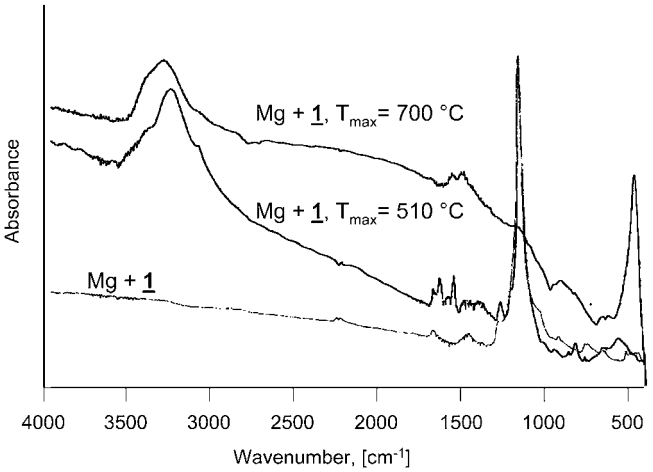

Figure 3. FTIR spectra of pyrolant and DSC residues

[17]. The residue from the DSC experiment heated to 700 °C reveals the complete disappearance of the tertiary C-F vibrations and the formation of a single strong signal at $\bar{\nu}$ =469 cm^{-1}, which is due to MgF_2.

The DSC experiments now prove for a pre-ignition reaction (PIR). Taking into account the Mg-C-vibration in Fig. 3 then the PIR may be described by Eq. (5).

Scheme 1 provides a sketch of the assumed decomposition mechanism of poly(carbon monofluoride) with magnesium.

On basis of this combustion model the increased reactivity of poly(carbon monofluoride) compared to poly(tetrafluoroethylene) can be explained.

The first reaction, that is Eq. (5) is an acid-base reaction of the type: A +:B → A ··B. Pearson has defined ΔN the number of electrons transferred from an electropositive partner :B (that is magnesium) to an electronegative partner A (that is the fluorocarbon) [18] as a measure for the rate constant of the acid-base reaction.

$$\Delta N = \frac{\chi_A - \chi_B}{2(\eta_A + \eta_B)}$$

with

χ_i = absolute electronegativity [eV],
η_i = hardness [eV].

Subscripts A and B refer to the acid and base. The values for χ_i and η_i can be calculated according to

$$\chi = \frac{IE + EA}{2}$$

$$\eta = \frac{IE - EA}{2}$$

with

IE = ionisation energy [eV], and
EA = electron affinity [eV].

Semi empirical calculation of the electronic properties (applying PM3 tool from HyperChem 7.0 [19]) both PTFE

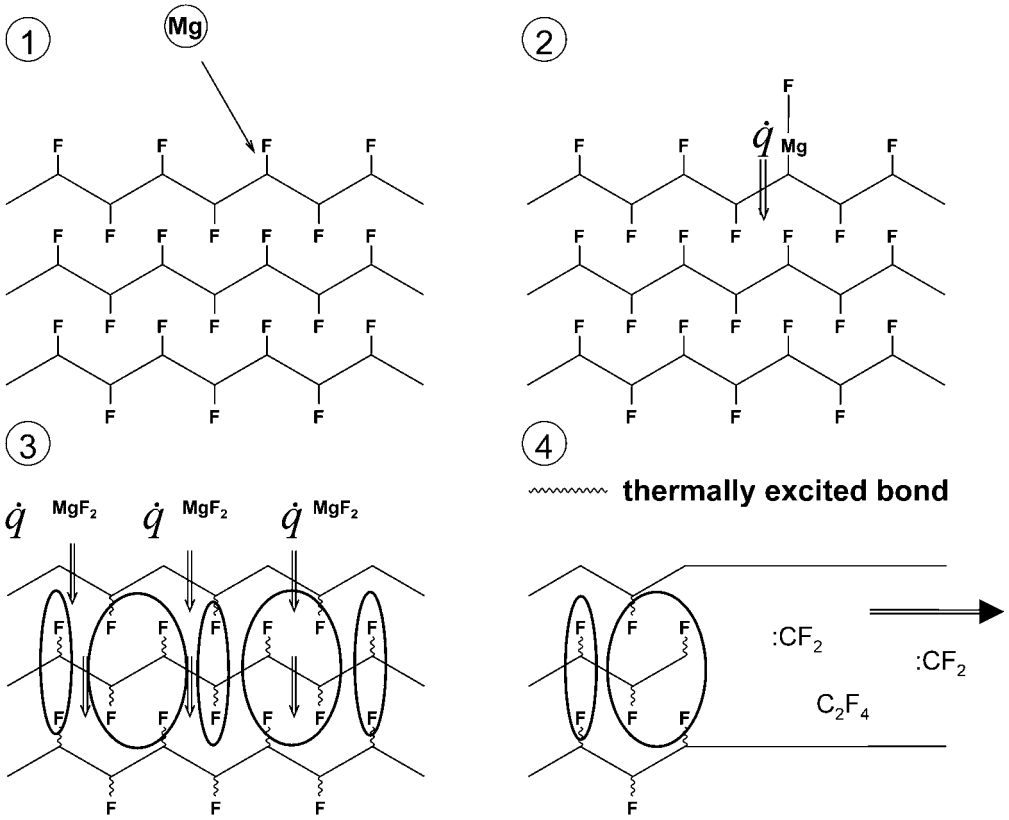

Scheme 1. Topochemical decomposition mechanism of poly(carbon monofluoride)

and PMF yields distinct differences in their highest occupied molecular orbital (HOMO) and lowest unoccupied molecular orbital (LUMO) energies which according to Koopmans' theorem [20] can be used to describe the ionization energy, *IE* and electron affinity, *EA*. ΔN for Mg/PTFE is 0.207 whereas ΔN for Mg/PMF is 0.243 [21] indicating the higher reactivity of latter system.

4 Investigation of Combustion Product of Pyrolant

From a strand prepared as described above (Section 3.1) a 5 mm long piece was cut and transferred to a stainless steel reaction vessel (5 L volume). The vessel was purged with argon gas (to impede carbon oxidation) for 5 min and the pyrolant piece was ignited with a Constantan™ wire to give a dazzling white flame and a dark smoke that precipitated on the bottom of the vessel.

Powder diffractometric analysis of the combustion products then revealed the presence of magnesium fluoride, graphite and structurally low ordered carbon [22].

Transmission electron microscopic (TEM) analysis of the combustion residues reveals the presence of spheroidal MgF_2 particles constituted from a large number of much smaller particles having diameters of approximately 20 – 40 nm thus calling for coalescence of melt liquid MgF_2 upon cooling Fig. 4a – b. These spherules are distributed randomly within exfoliated graphite and Carbon Nano Carpet Rolls (CNCR). The formation of both has been observed likewise upon thermal treatment of graphite fluoride in inductively coupled argon plasma [23]. CNCR form when the reconstituted graphite sheet is forced to roll. This may be due to thermal excitation of graphite but has not been observed with pristine graphite so far under likewise conditions.

Removal of MgF_2 by washing the combustion residue with hot Na_2CO_3 solution and successive treatment with hot HCl and demineralised water to wash away NaF leaves exfoliated graphite, soot and Single Wall Carbon Nanotubes (SWCNT) [24].

Thermochemical analysis of the combustion of said stoichiometry (40/55/5) applying NASA CEA code [25] reveals major amounts of graphite and unburnt magnesium in the anaerobic zone, Fig. (6). With rising weight fraction of entrained air at first the combustion temperature declines, Fig (5). At first sight this looks anomalous but is easily explained looking at the chemical equilibria taking place between of $Mg/CO/CO_2$ [26 – 28]. In the stoichiometric range $\xi(\text{air}) < 0.6$ oxidation of Mg by CO does not take place since for the reaction $Mg + CO = MgO + C$ $\Delta G > 0$. At $\xi(\text{air}) > 0.6$ CO_2 reacts with Mg to give CO and MgO and the temperature again rises steep to reach ~2800 K. After consumption of both CO and Mg the temperature declines again. Now no significant exothermal reactions take place and the decline in temperature is a consequence of dilution of the combustion products with cool air.

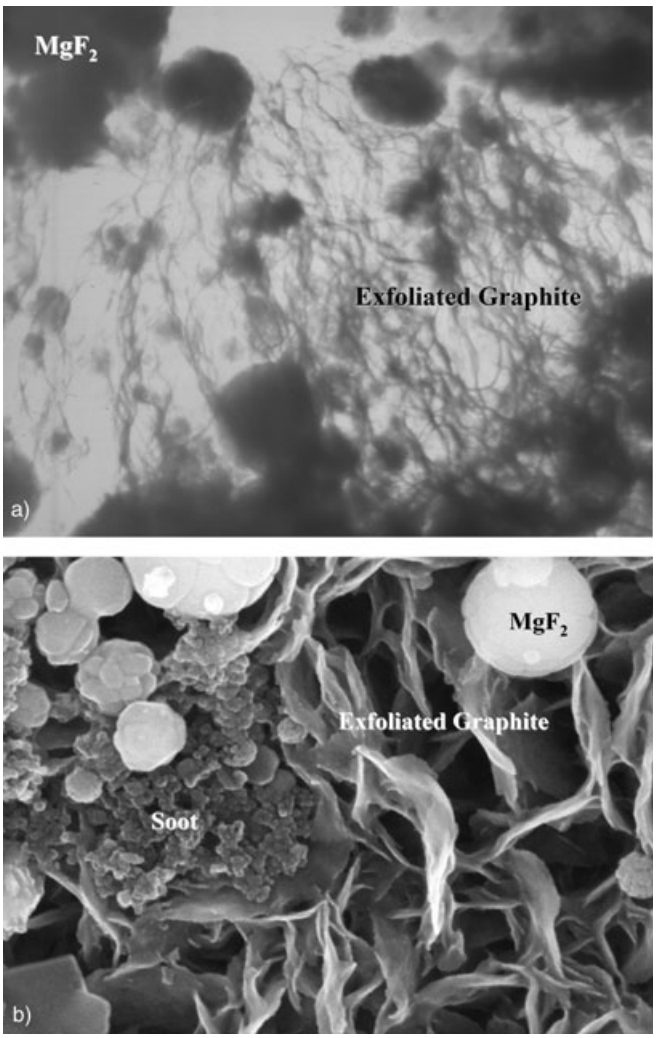

Figure 4. TEM a) and HREM b) picture of combustion product

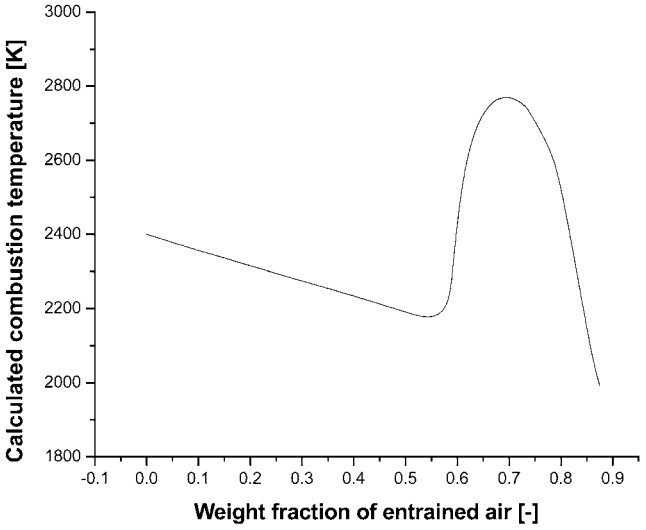

Figure 5. Composition as function of entrained air

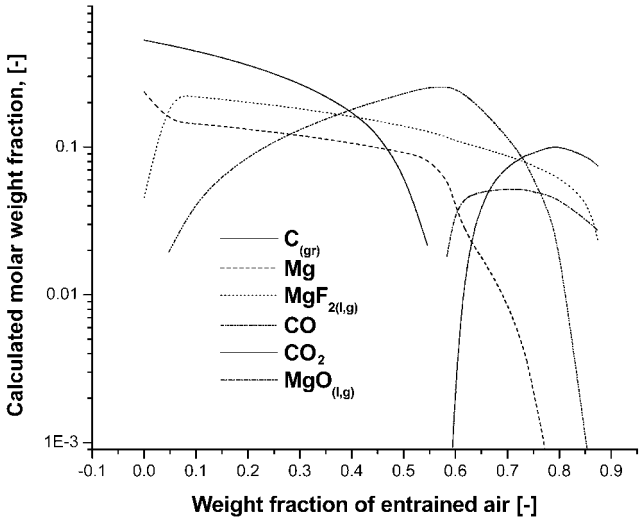

Figure 6. Combustion temperature as function of entrained air

5 Radiative and Thermochemical Properties of Pyrolant

The specific intensity, E_λ, of an IR-emitting pyrolant is given by the following equation:

$$E_\lambda = \frac{1}{4\pi} \Delta_c H \cdot F_{\lambda,T} \cdot d_w \left[\mathrm{J\ g^{-1}\ sr^{-1}}\right] \tag{7}$$

with

$\Delta_c H$ = the enthalpy of combustion of the pyrolant [J g^{-1}],
$F_{\lambda,T}$ = the fraction of radiation in the band of interest [–],

In addition the specific intensity of a pyrolant is further influenced by wind stream effects [29]. Thus the wind stream degradation factor, d_w [–], accounts for the decrease in specific intensity with values ranging from 1.0 at static to 0.3 at 100 m s^{-1} and ~0.1 at 300 m s^{-1} conditions. This decrease in intensity at higher wind speed is mainly due to decrease of luminous zone due to gas dynamic effects.

The fraction of the radiation in the band of interest is determined by:

$$F_{\lambda,T} = \frac{1}{\varepsilon\sigma T^4} \frac{\varepsilon C_1}{\lambda^5} \int \frac{1}{e^{\left(\frac{C_2}{\lambda T}\right)}_{-1}} d\lambda \tag{8}$$

ε = the average emissivity [-],
σ = the Stefan-Boltzmann constant, $5.67 \cdot 10^{-8}$ [W m^{-2} K^{-4}],
T = the combustion temperature [K],
λ = the wavelength [μm],
C_1 = the 1st Planck radiation constant, $3.7418 \cdot 10^{-16}$ [W m^2] and
C_2 = the 2nd Planck radiation constant, $1.4388 \cdot 10^{-2}$ [m K].

Thus the specific intensity E_λ is mainly dependent on the emissivity of the combustion products ε and the enthalpy of combustion $\Delta_c H$ of the pyrolant. Furthermore an additional figure of merit is the mass consumption rate $\dot{m}$[g s^{-1} cm^{-2}] since

$E_\lambda \cdot \dot{m} = I_\lambda$ [W sr^{-1}]

with

I_λ = the pointance [W sr^{-1} cm^{-2}] and

$\dot{m}$ = mass consumption rate [g s^{-1} cm^{-2}]

To alter the performance of an infrared radiation pyrolant either the specific intensity and/or the mass consumption rate have to be enhanced.

The remaining pyrolant strand (vide infra) was fixed between steel splint pins having square geometry on a brass cylinder and was equipped with a black powder quick match fixed on top. The lateral surfaces of the pellet were wrapped with adhesive Kraft-paper. The combustion of the pellet was recorded with circular variable filter spectroradiometer with liquid nitrogen cooled InSb detector (SR 5000, Polytec, Waldbronn/Germany, scanrate: 100 Hz, FOV: 6 mrad, CVF-time: 0.1 s, chopper frequency: 1800 Hz) after calibration with a blackbody of temperature 1000 K (SR-32-SR, CI-Electro-Optics Systems, Haifa/Israel). In addition radiometric measurements were made with two channel IR radiometric system (RM 6600, Polytec, Waldbronn/Germany; uncooled pyroelectric detector RkP575). All measurements were done from 10 m distance in a test tunnel allowing for a constant stream of air toward the pyrolant strand equipped with a suction fan placed above the pyrolant strand ($v_{static} = 3$ m s^{-1}).

Fig. 7 displays the spectrally resolved spectral radiant exitance of the pyrolant. The spectrum is mainly determined by the continuum radiation of the graphite. The continuum is further superimposed from molecular bands of H_2O, HF, CO_2 and CO. The envelope of the curve can be fitted with reasonable accuracy by a blackbody of T = 2700 K having $\varepsilon = 1.0$. As has been mentioned above wind stream effects degrade the specific radiant exitance of pyrolant flames [30]. Pyrolant strands of the above type have been investigated at different wind speeds up to 125 m s^{-1}. Fig. 8 displays the specific intensity for both 2–3 μm and 4–5 μm band. With increasing wind speeds the intensity in 2–3 μm band decreases significantly. Although specific intensity in 4–

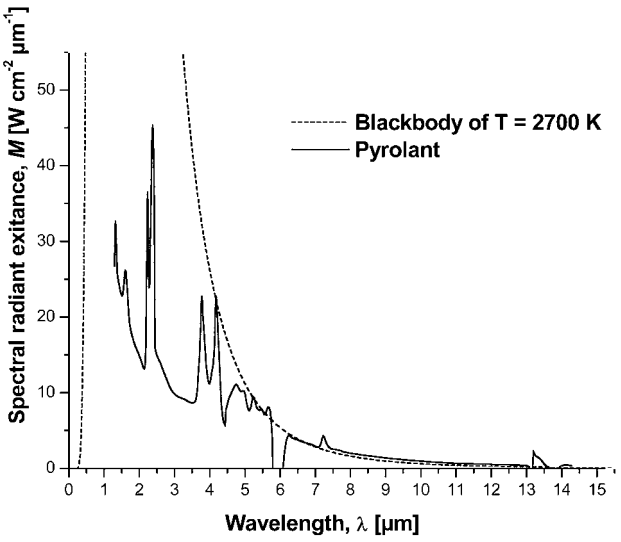

Figure 7. Spectral radiant exitance of pyrolant and blackbody having $T = 2700$ K

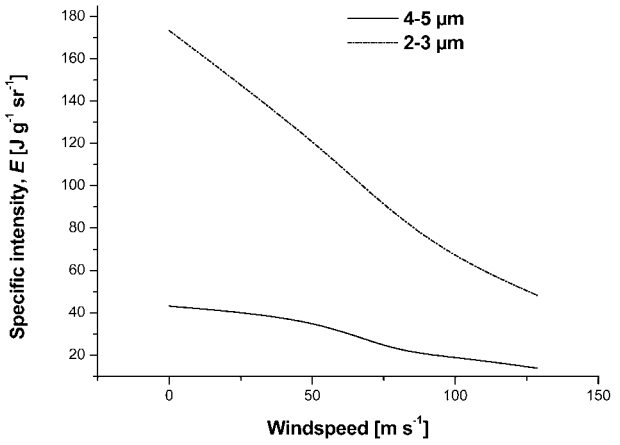

Figure 8. Specific intensity E_λ of pyrolant under static and dynamic conditions at two bands

Table 2. Properties of magnesium/poly(carbon monofluoride)/Viton™ and magnesium/poly(tetrafluoroethylene)/Viton™ pyrolant

Parameter	Unit	MTV	MPV
Magnesium	wt%	40	40
Poly(tetrafluoroethylene)	wt%	55	–
Poly(carbon monofluoride)	wt%	–	55
Hexafluoropropylene Vinylidene fluoride Copolymer	wt%	5	5
$\Delta_{anaerobic}H^\circ$	kJ kg^{-1}	−12962	-10569
$\Delta_{aerobic}H^\circ$	kJ kg^{-1}	−20545	-22080
$E_{2-3\ \mu m}$	kJ kg^{-1} sr^{-1}	103	170
$E_{3-5\ \mu m}$	kJ kg^{-1} sr^{-1}	80	157
$I_{2-3\ \mu m}$	kW sr^{-1} cm^{-2}	0.072	0.511
$I_{3-5\ \mu m}$	kW sr^{-1} cm^{-2}	0.056	0.472
m	g s^{-1} cm^{-2}	0.7	0.303
r	mm s^{-1}	3.643	16.013
$\rho_{20^\circ C}$	g cm^{-3}	1.92	1.876
ΔN	1	0.207	0.243

$\Delta_{anaerobic}H$: enthalpy of combustion under anaerobic conditions; $\Delta_{aerobic}H$: enthalpy of combustion under aerobic conditions; E_{2-3} μm, E_{3-5} μm: specific intensity at selected waveband; I_{2-3} μm, I_{3-5} μm: pointance at selected waveband; $\dot{m}$: mass consumption rate; r: linear burn rate; ΔN: number of electrons transferred.

5 μm decreases likewise the decline especially in the speed range between 0 – 50 m s^{-1} is not as pronounced as in the 2 – 3 μm band.

6 Conclusion

The advantageous properties of graphite fluoride as an oxidizer in infrared radiation pyrolants in comparison to poly(tetrafluoroethylene) are the following:

- the formal defluorination of poly(carbon monofluoride) yields graphite the only material showing the highest emissivity in the infrared spectral range at combustion temperatures [31] thus enhancing specific intensity, E_λ ,
- the lower enthalpy of formation, $\Delta_f H^\circ$, of graphite fluoride compared to poly(tetrafluoroethylene) provides a higher combustion enthalpy with magnesium,
- graphite fluoride also exhibits a faster rate of reaction thus enhancing the mass consumption rate $\dot{m}$ [1] which in turn provides a higher pointance I_λ.

Table 2 provides a synopsis of both $\xi(\mathrm{Mg}) = 0.40$ based PTFE and PMF based pyrolants.

7 References

[1] E.-C. Koch, Metal/Fluorocarbon Pyrolants, V, Theoretical Evaluation of the Combustion Performance of Metal/Fluorocarbon Pyrolants based on Strained Fluorocarbons, *Propellants, Explos., Pyrotech.* **2004**, *29*, 9.

[2] E.-C. Koch, Review on Pyrotechnic Aerial Infrared Decoy Flares, *Propellants, Explos., Pyrotech.* **2001**, *26*, 3.

[3] E.-C. Koch, Metal/Fluorocarbon Pyrolants, III, Development and Application of Magnesium/Teflon/Viton(MTV), *Propellants, Explos., Pyrotech.* **2002**, *27*, 262.

[4] P. Gongpei, W. Xue, L. Yi, The Influence of PTFE Effective Mass Flow Rate on 3 – 5 μm Radiant Intensity in Mg/PTFE/BaO_2 Infrared Pyrotechnic Composition, *24th International Pyrotechnics Seminar*, Monterey, USA, July 27 – 31, **1998**, pp. 607 – 612.

[5] P. Gongpei, Z. Chang-jiang, W. Xue, L. Yi, Factors influencing on the Radiant intensity of Infrared Radiation Pyrotechnics, *J. Ener. Mater.* **1999**, *7*, 57.

[6] E.-C. Koch, A. Dochnahl, IR Emission Behaviour of Magnesium/Teflon/Viton Composition, *Propellants, Explos., Pyrotech.* **2000**, *25*, 37.

[7] E. Kujala, T. Kaurila, Radiometric Measurements on Infrared Flares, *FINNEX2002*, Levi, Finland, September 9 – 11, **2002**, 219.

[8] D. L. Cohen, A Model for the Infrared Radiance of Optically-Thin, Particulate Exhaust Plumes Generated by Pyrotechnic Flares Burning in a Vacuum, *Technical Report 821*, Lincoln Laboratory, Massachusettes Institute of Technology, 17 March 1989, reissued 29 March **2000.**

[9] O. A. Alekseev, Model of the Radiation of the Flares of Pyrotechnic Thermal Decoy, *J. Opt. Techol.* **2004**, *71*, 94.

[10] E.-C. Koch, Poly(kohlenstoffmonofluorid) ein Extrem Energiereiches Oxidationsmittel, *10. GDCh Vortragstagung – Anorganische Funktionsmaterialien* – 26.-29. September **2000**, Münster, p. A-62.

[11] T. K. Liu, I.-M. Shyu, Y. S. Hsia, Effect of Coating Boron with CFx and its Agglomeration and Combustion Characteristics of Fuel-Rich Propellants, *Taiwan. J. Chem.* **1993**, *9*, 9.

[12] T.-K- Liu, I.-M. Shyu, Y.-S. Hsia, Effect of Fluorinated Graphite on Combustion of Boron and Boron-Based Fuel-rich Propellants, *J. Propul. Power* **1996**, *12*, 26.

[13] J. L. Fields, J. D. Martin, Patent US6736912, **2004**, USA.

[14] P. Kamarchik Jr., J. L. Margrave, Poly(carbon monofluoride) – a Solid Layered Fluorocarbon, *Acc. Chem. Res.* **1978**, *11*, 296.

[15] E.-C. Koch, Patent US6635130, **2003**, Diehl Munitionssysteme GmbH & Co. KG, Deutschland.

[16] N. Watanabe, T. Nakajima, H. Touhara, *Graphite Fluorides*, Elsevier Publishers, Amsterdam **1988**, 122.

[17] E.-C. Koch, Metal-Fluorocarbon Pyrolants. IV: Thermochemical and Combustion Behavior of Magnesium/Teflon/Viton (MTV), *Propellants, Explos., Pyrotech.* **2002**, *27*, 340.

[18] R. G. Pearson, *Chemical Hardness*, Wiley-VCH, Weinheim **1997**, 29 – 38.

[19] *HyperChem 7.0*, Molecular Visualization and Simulation Program Package, Hypercube, Inc., Gainsville, FL, **2002.**

[20] T. M. Klapötke, A. Schulz, *Quantum Chemical Methods In Main Group Chemistry*, John Wiley, New York **1998**, 41.

[21] E.-C. Koch, Acid-Base Interactions in Energetic Materials. I: The Hard and Soft Acids and Bases (HSAB) principle, *Propellants, Explos., Pyrotech.* **2005**, *30*, 5.

[22] E.-C. Koch, Fluoreliminierung aus Graphitfluorid mit Magnesium, *Z. Naturforsch. B: Chem. Sci.* **2001**, *56*, 512.

[23] T. J. Manning, M. Mitchell, J. Stach, T. Vickers Synthesis of Exfoliated Graphite from Fluorinated Graphite Using an Atmospheric-Pressure Argon Plasma, *Carbon* **1999**, *37*, 1159.

[24] E.-C. Koch, Patent DE 10122750, Diehl Stiftung, **2001**, Germany

[25] S. Gordon, B. J. McBride, Computer Program for Calculation of Complex Chemical Equilibrium Compositions and Applications, *NASA Reference Publications 1311*, **1994.**

[26] S. Yuasa, A. Fukuchi, Ignition and Combustion of Magnesium in Carbon Dioxide Streaks, *25th Int. Sympos. Combustion*, **1994**, 1587.

[27] A. Fukuchi, M. Kawashima, S. Yuasa, Combustion Characteristics of Mg-CO_2 Counterflow Diffusions Flames, *26th Int. Sympos. Combustion*, Naples, Italy, **1996**, 1945.

[28] A. Abbud-Madrid, A. Modak, M. C. Branch, J. W. Daily, Combustion of Magnesium with Carbon Dioxide and Carbon Monoxide at Low Gravity, *J. Propul. Power* **2001**, *17*, 852.

[29] N. Brune, *Expendable Decoys*, in J. S. Accetta, D. L. Shumaker, *The Infrared and Electro-Optical Systems Handbook*, Vol. 7, 305 – 306, SPIE Optical Engineering Press, Bellingham **1996.**

[30] N. Davies, D. A. Holley, Factors Affecting the Radiometric Output of Infrared Flares, *22th , International Pyrotechnics Seminar*, Fort Collins, USA, July 15 – 19, **1996**, 469.

[31] A. J. LaRocca, *Artificial Sources*, in J. S. Accetta, D. L. Shumaker, *The Infrared and Electro-Optical Systems Handbook*, Vol. 1, 112, SPIE Optical Engineering Press, Bellingham **1996.**

(Received August 25, 2004, Ms 2004/028)

